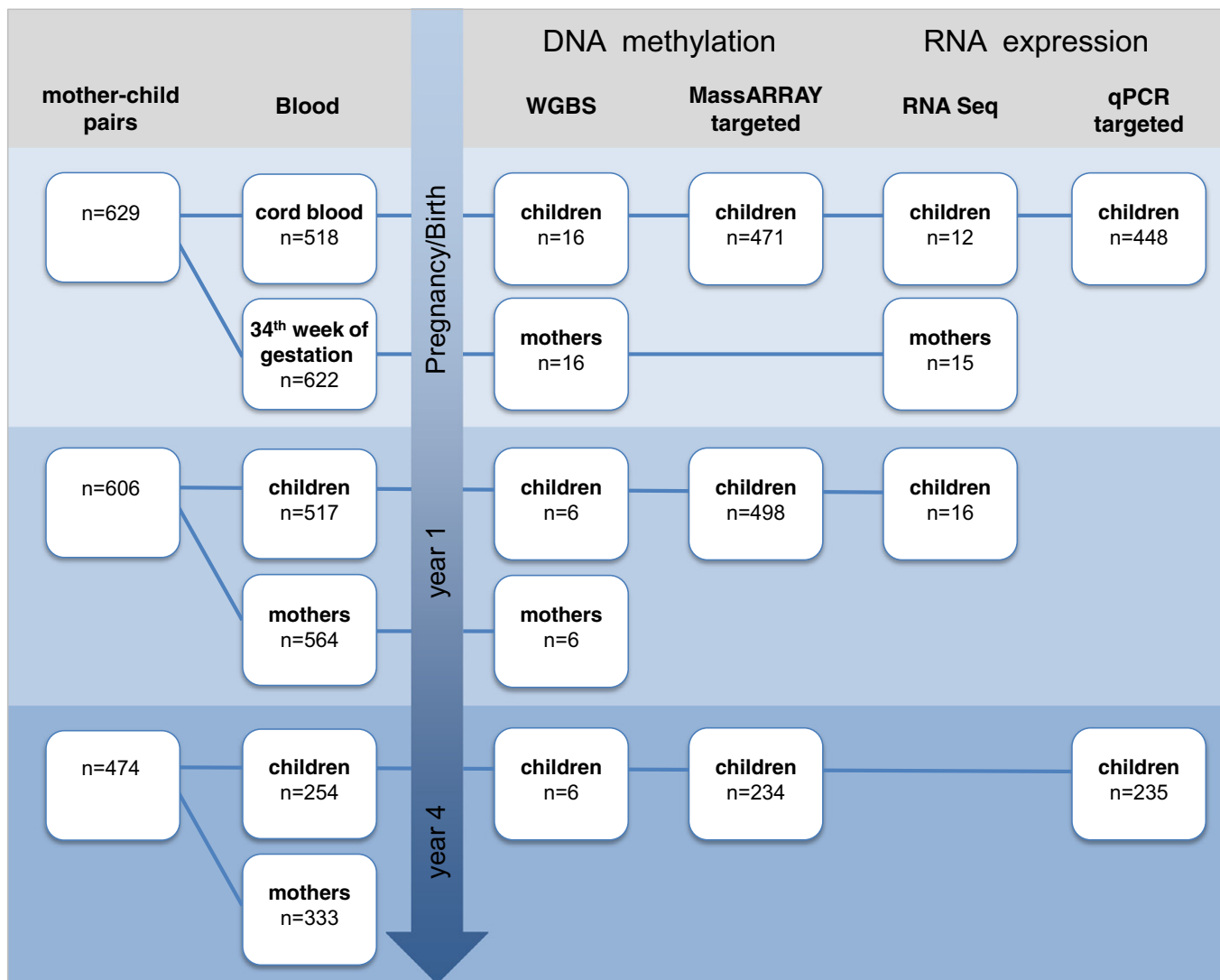
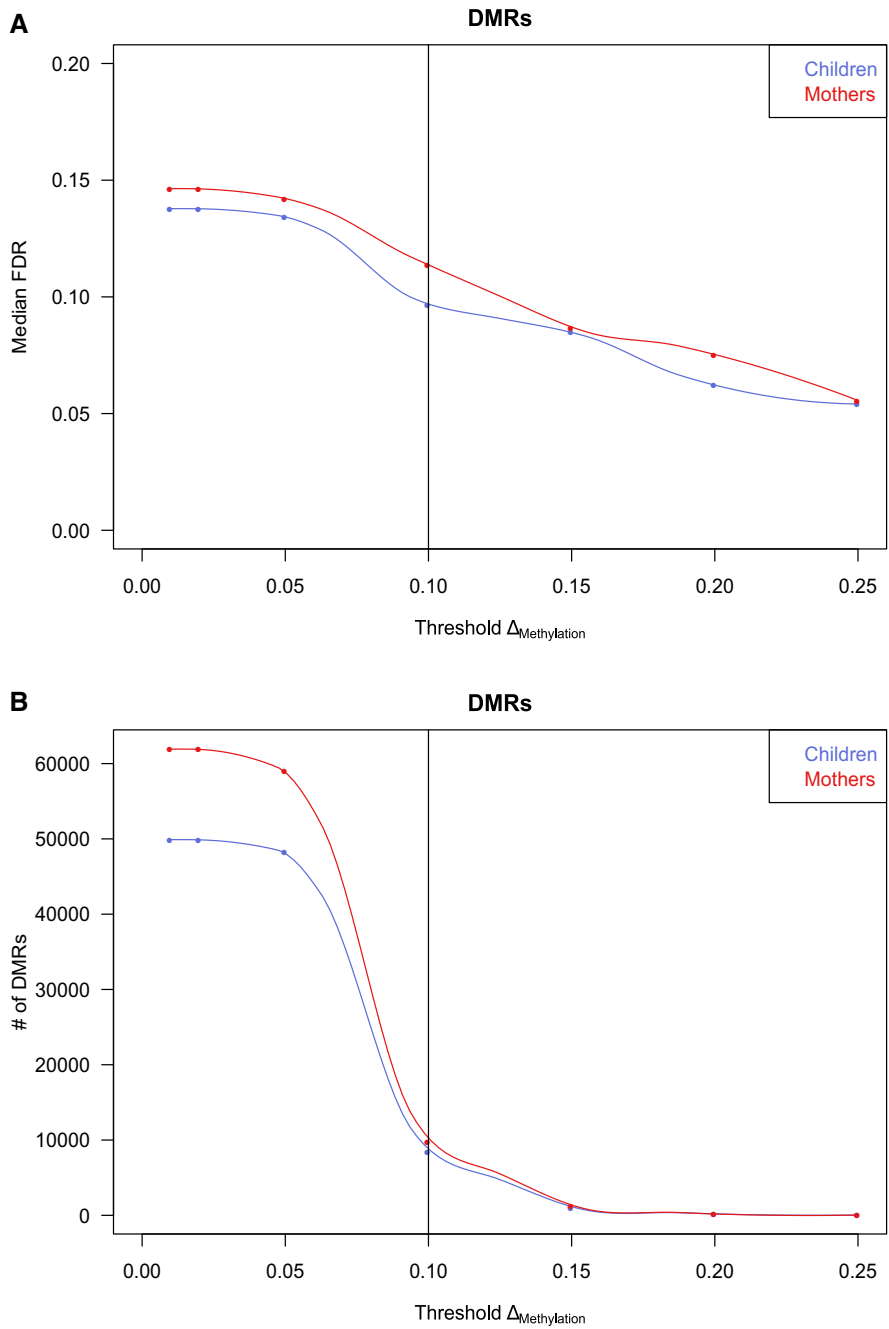


### Expanded View Figures



**Figure EV1. Cohort and sample overview.**

The diagram visualizes the number of mother-child pairs enrolled in the study together with the number of available blood samples (left). For the different experimental approaches, the number of samples analyzed is given starting at time of birth/pregnancy up to year 4 after birth (right).



**Figure EV2. FDR and number of DMRs at different methylation difference thresholds.**

A Median false discovery rate (FDR) estimated by permutation analysis at different cutoffs for mean methylation changes of DMRs ( $\Delta_{\text{Methylation}}$ ).  
 B Number of DMRs after filtering called at different mean methylation changes. The 10%  $\Delta_{\text{Methylation}}$  cutoff is marked and indicates a fair balance between sensitivity and specificity while offering acceptable FDRs (9.7% in children, 11.4% in mothers).

**Figure EV3. meQTL distinguish gDMR and ngDMR.**

A–D Each DMR is associated with its most highly associated SNP within  $\pm 5$  kb, and each dot represents a DMR/SNP association. The x-axis shows the level of correlation between genotype and methylation level, and the y-axis shows the methylation difference for the DMR between the smoking and non-smoking group. DMRs associated with a CpG-destroying SNP are highlighted in green. A gDMR is defined as a DMR, which has an associated neighboring SNP with an absolute correlation above 0.6 (red vertical lines, FDR 10%), and the remaining DMRs are defined as ngDMRs (red shaded area). The effect of the 10% cutoff on the methylation difference is seen in this plot. Violin plots in (B, D) show the methylation difference in all DMRs, ngDMRs, and gDMRs.  
 E, F Methylation differences are shown for the various DMR stability classes, distinguishing ngDMRs (left in violin plot pairs) from gDMRs (right violin plot in each pair).

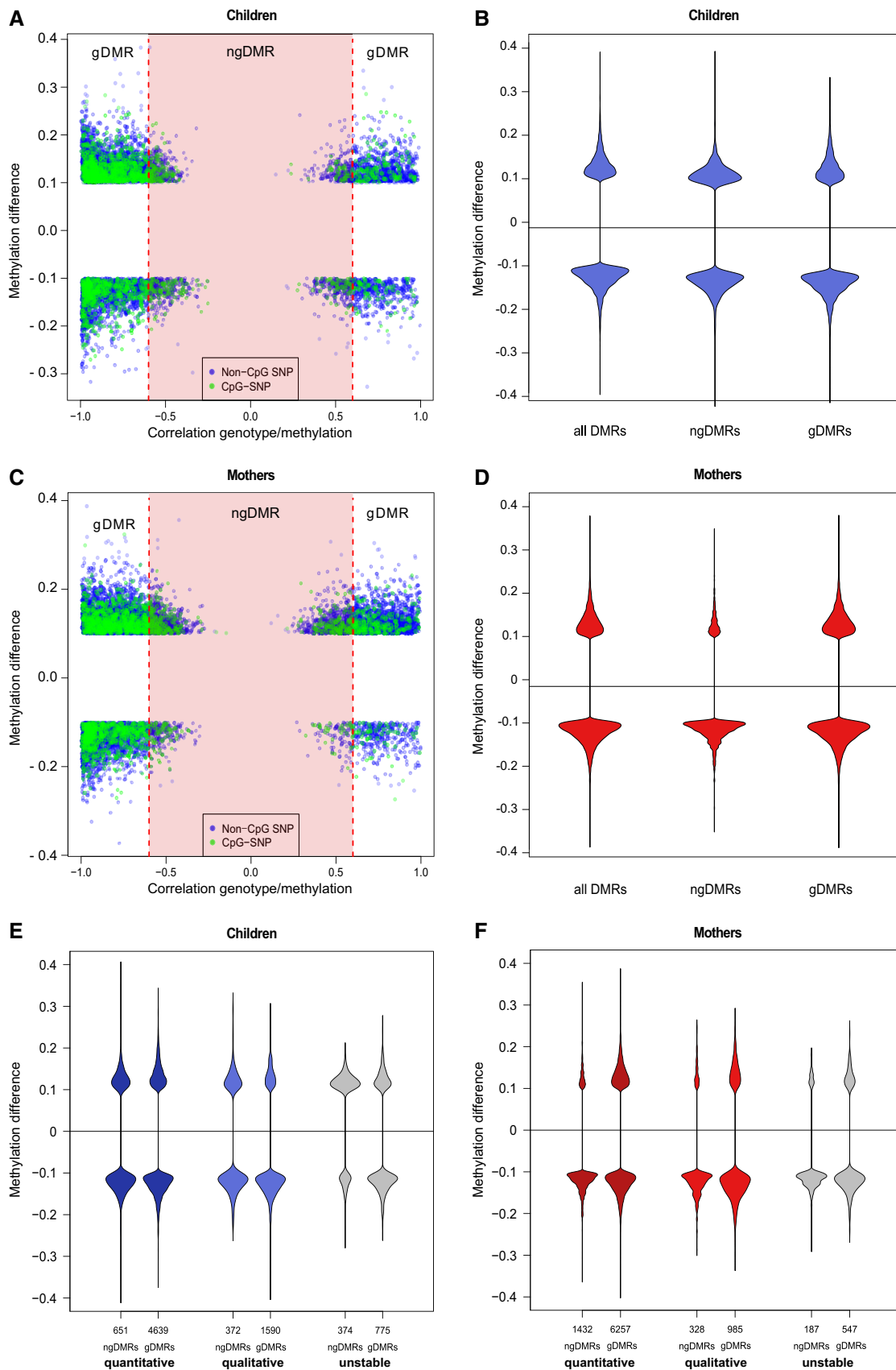
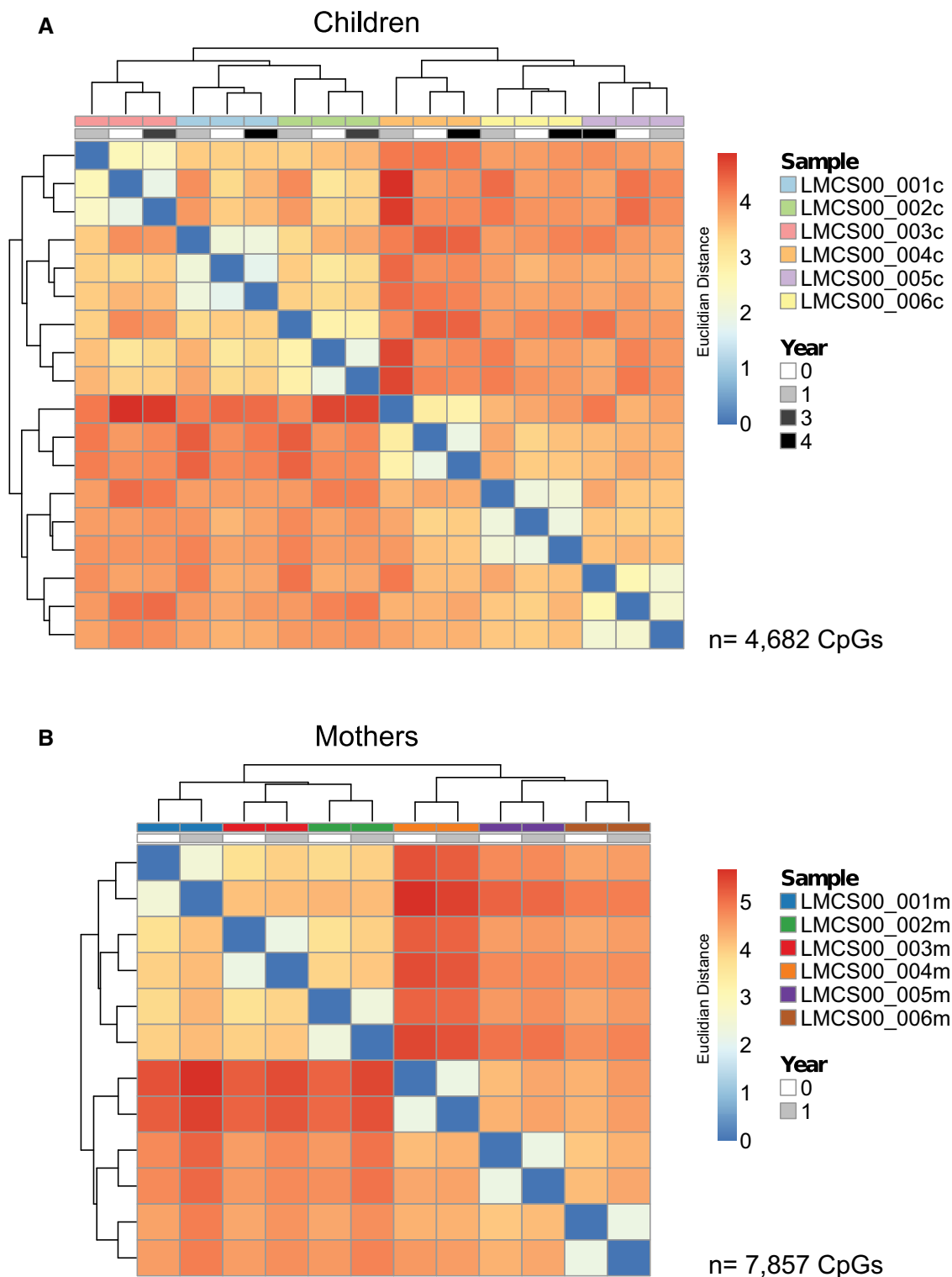
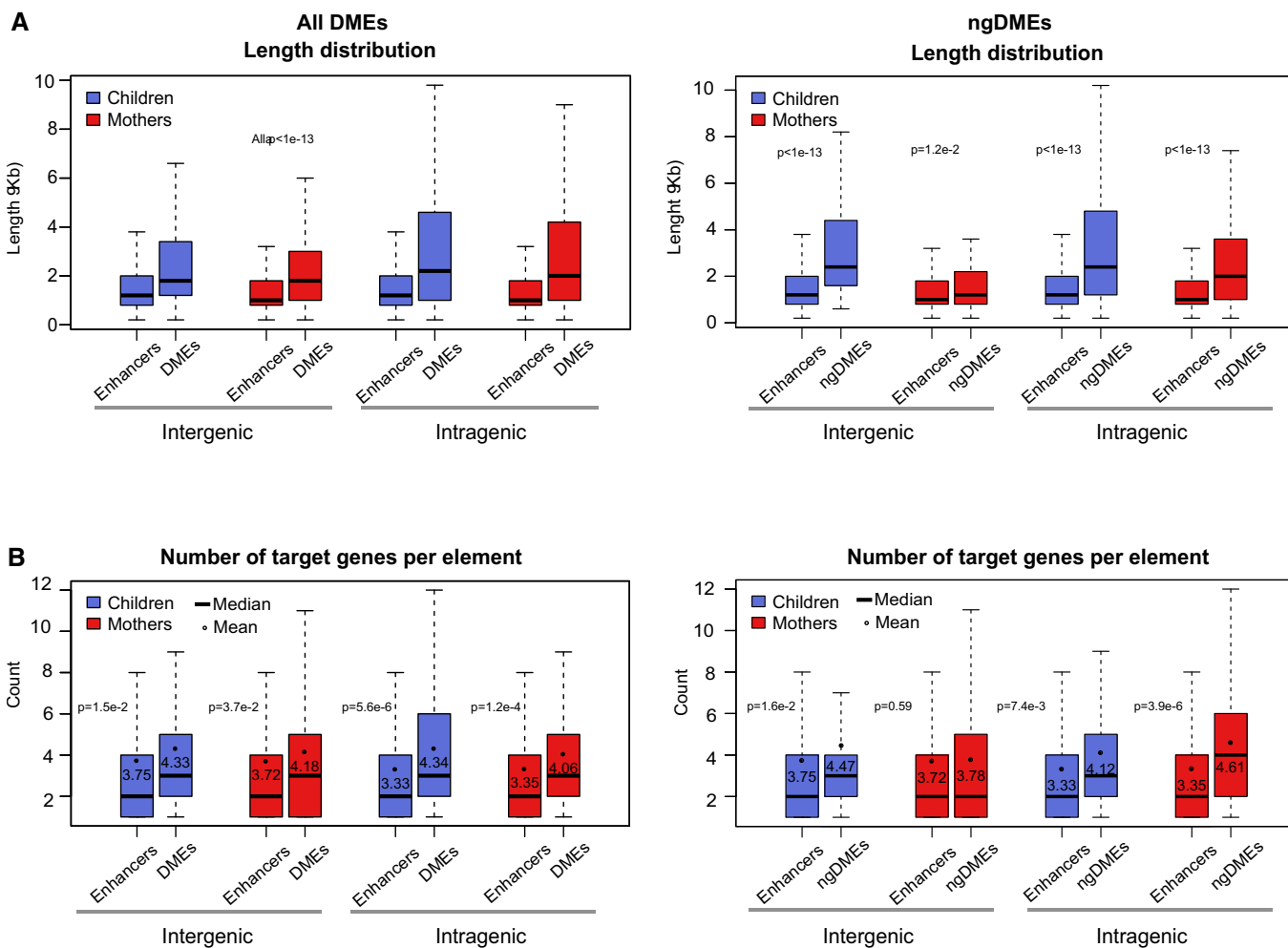


Figure EV3.



**Figure EV4. Temporal DMR stability assessment by clustering DNA methylation of CpGs in ngDMRs.**

A, B Hierarchical clustering (Euclidean distance) of methylation of all CpGs in ngDMRs that are not subject to SNPs in any sample. Only CpGs with a minimum coverage of 10 reads in all samples were considered. Clustering occurs by sample, not by year, suggesting high maintenance of CpG methylation levels for each sample over time. (A) Children (n = 4,682 CpGs), (B) mothers (n = 7,857 CpGs).



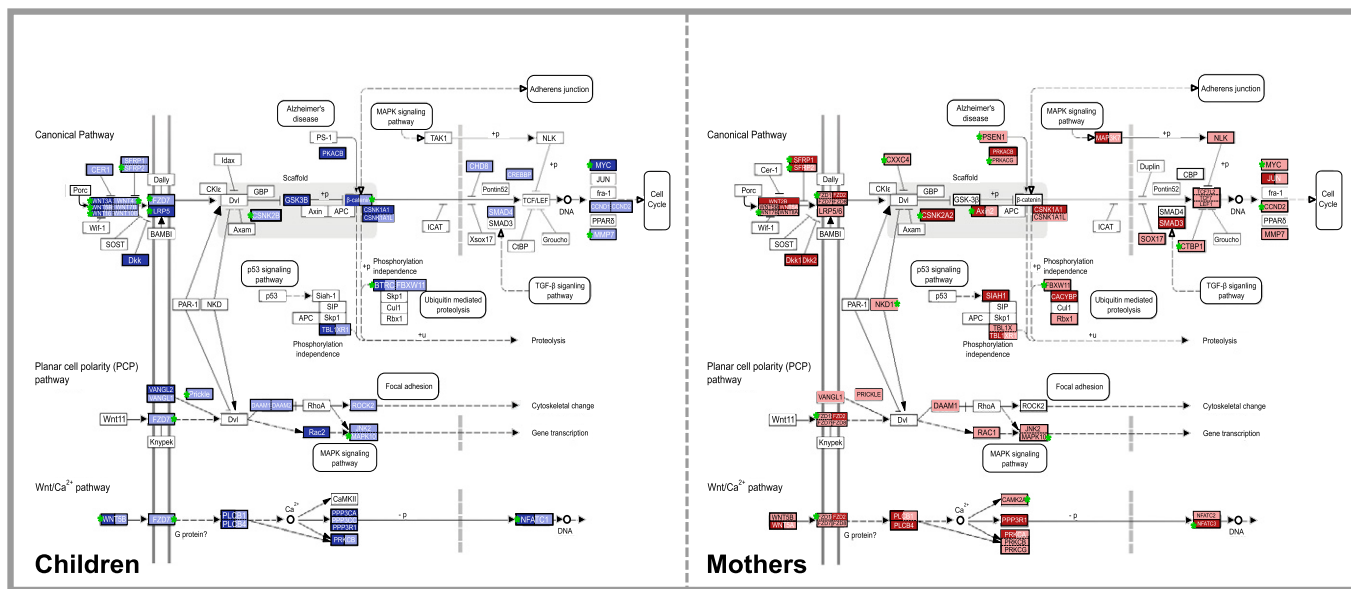
**Figure EV5. Differentially methylated enhancers are regulatory hubs.**

A Length distribution of enhancers (non-TSS-associated active regulatory regions) and ngDMEs in mothers and children, both inter- and intragenic, indicating a significant increase in length for differentially methylated enhancers compared to other enhancers.

B Distribution of the number of predicted target genes from the interaction datasets for the same categories as in (A). Black dots indicate the mean number. The corresponding *P*-value is indicated (Mann–Whitney test), showing a significant increase for ngDMEs, which is more pronounced in intragenic elements.

Data information: (A, B) Box plots visualize 25/75 percentile and median, whiskers represent non-outlier range.

WNT SIGNALING PATHWAY



\*ngDMR

Figure EV6. Perturbation of the WNT signaling pathway.

Shown are modified outputs of the KEGG Mapper tool (v2.1, April 2014) of the WNT signaling pathway for DMRs identified in mothers and children during pregnancy and at time of birth, respectively. Each DMR assigned to a gene of this pathway is indicated in blue for children or red for mothers. The lighter hues correspond to hypomethylation, while the darker hues indicate hypermethylation. Green stars denote DMRs classified as ngDMRs.

Figure EV7. Differential methylation impacts the expression of downstream pathways.

- A The bar plot shows the list of pathways that are significantly enriched among the target genes of DMRs intersecting active enhancers and promoters both in mothers and in children (enrichment *q*-value indicated on *x*-axis) and that show differential expression of genes between smoking and non-smoking samples as measured by RNA-seq in either children or mothers. Color of bars indicates significance of differential expression of genes in this pathway (see Appendix Supplementary Methods for details of the calculation). Note that the WNT pathway shows the strongest differential expression in children.
- B WNT signaling genes interacting with differentially methylated enhancers (DMEs) show clustering of smokers versus non-smokers from the RNA expression profile (DME target prediction was mapped by ChIA-PET where available and nearest TSS otherwise).

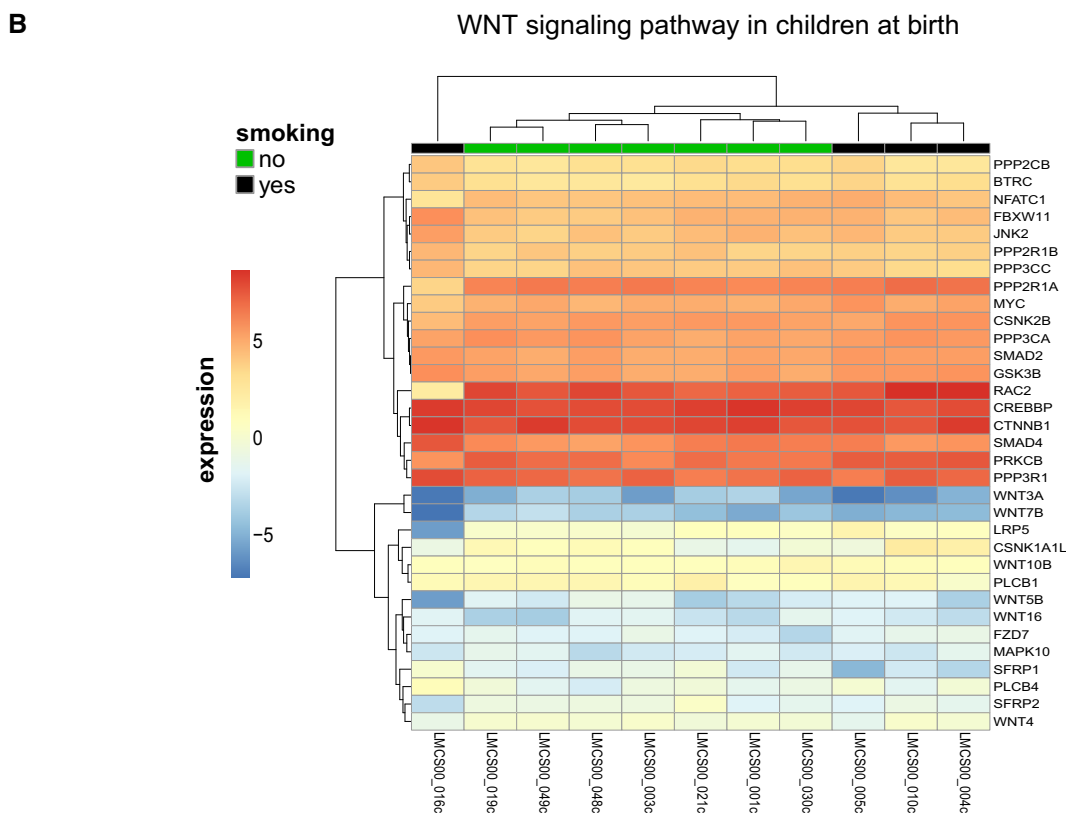
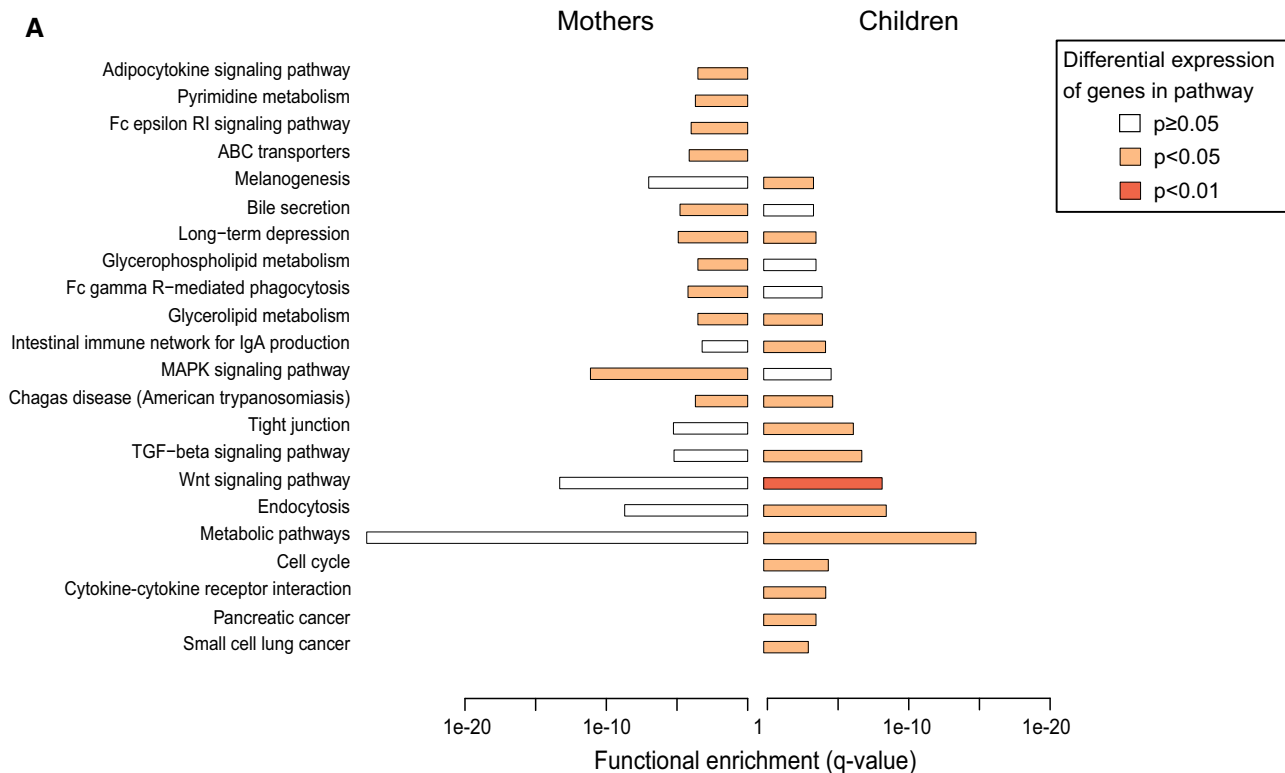
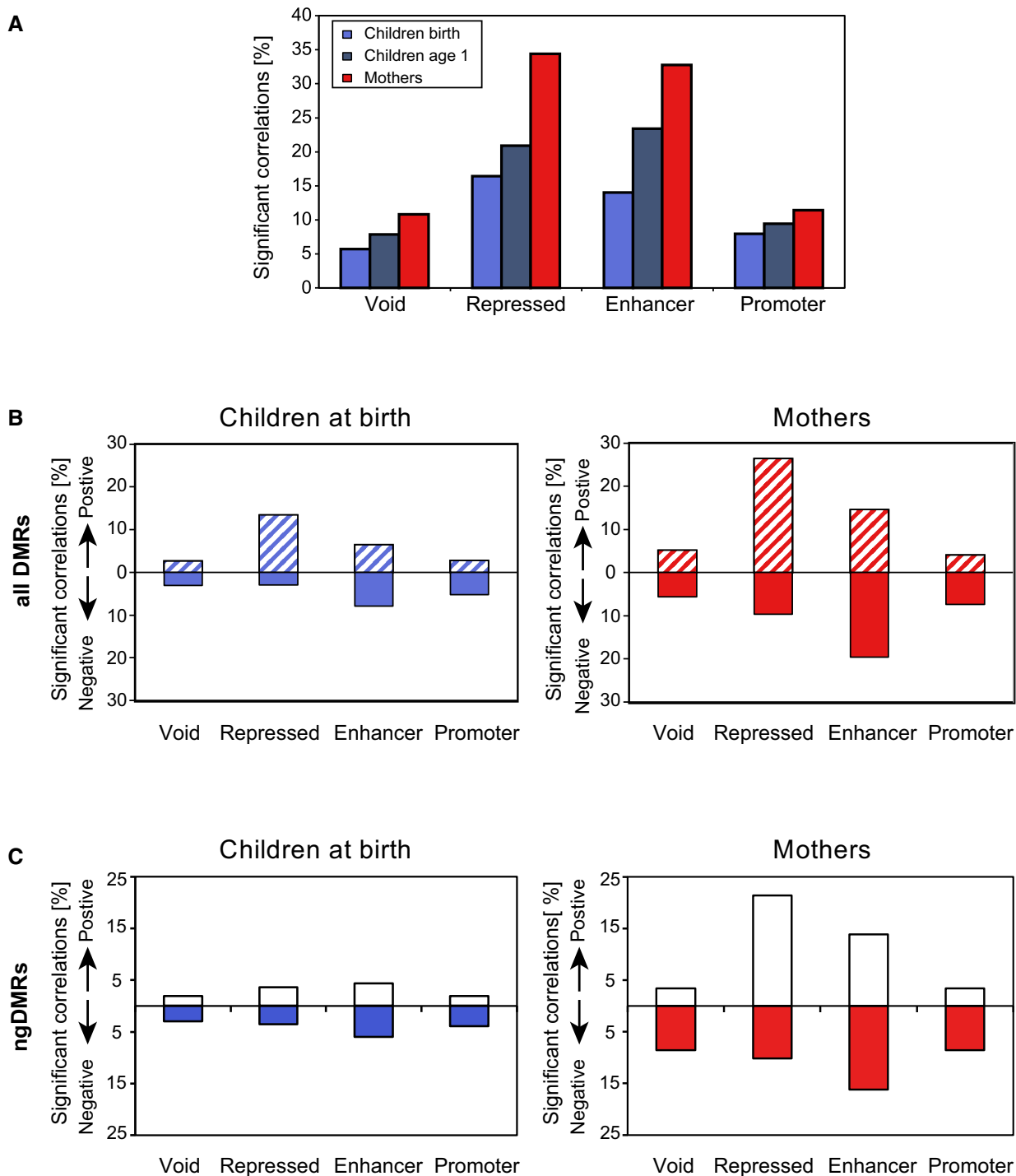


Figure EV7.



**Figure EV8. Correlation of differential methylation and transcription in regulatory elements.**

A Proportion of DMR-target gene pairs showing a significant correlation (Spearman's correlation test  $p < 0.05$ ) between mean methylation and target gene expression, indicating a higher correlation level for DMRs in repressed or enhancer regions as compared to void or promoter regions. Also, correlation levels increase for children from year 0 to year 1 indicating a temporal gap between epigenetic changes and induced gene expression.

B Proportion of significantly correlated DMR-target gene pairs in the same categories as (A), split into positive/negative correlation, showing an excess of positive correlation for DMRs associated with repressed regions (containing one or both PRC-associated H3K27me3 marks as well as the repressive H3K9me3 marks), and an excess of negative correlations for active regions (enhancers and promoters).

C Proportion of significantly correlated ngDMR-target gene pairs split into positive/negative correlation in the same categories as (B).



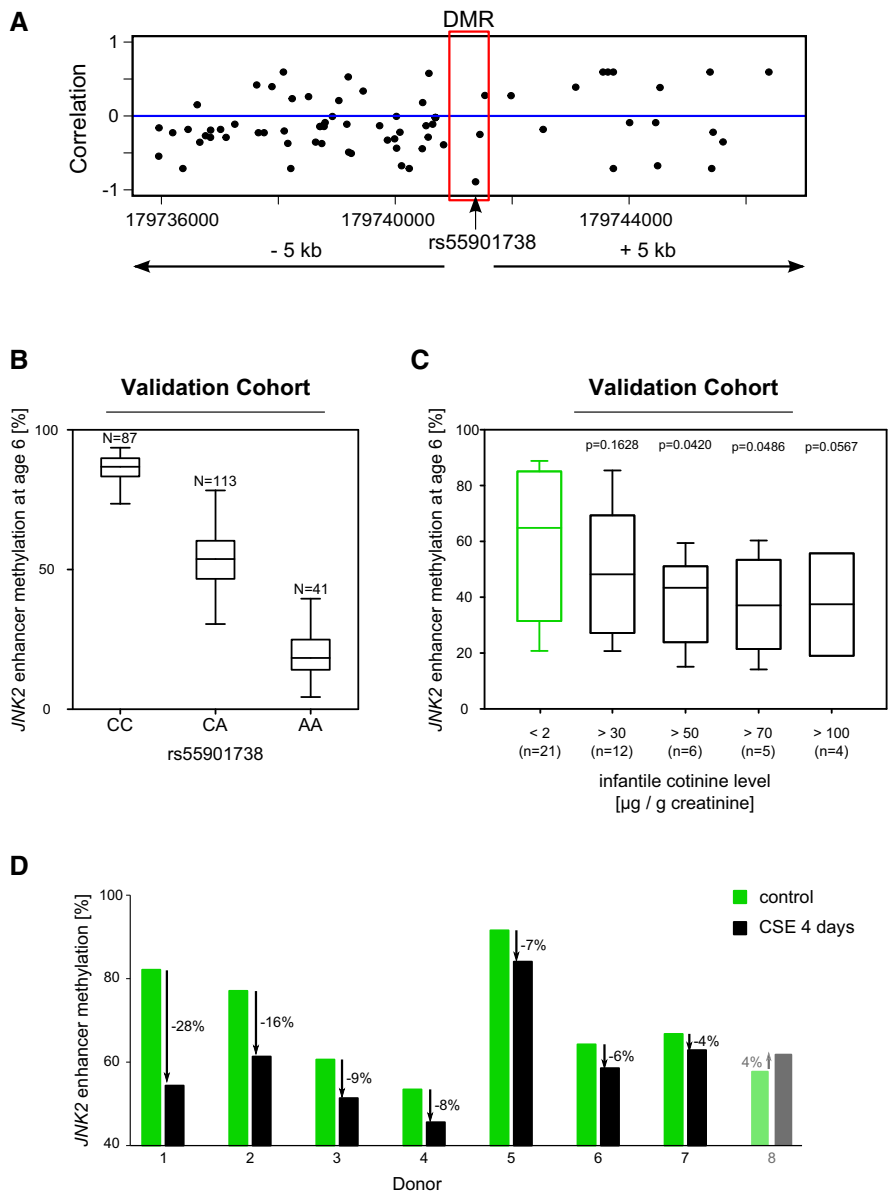


**Figure EV9. Genotype and tobacco smoke exposure influence methylation of the JNK2 commuting enhancer.**

- A Locus around the JNK2 DMR showing for each genotyped SNP the correlation of the genotype to the methylation in the DMR region.
- B Genotype at the SNP rs55901738 located inside the DME in the validation cohort (N = 87/113/41) indicating a clear negative correlation between the genotype and the methylation level at this locus.
- C In an independent validation cohort, we confirmed in six-year-old children that cigarette smoke exposure (passive smoking) leads to a decrease of methylation in the JNK2 enhancer region. Children's urine cotinine levels inversely correlate with the JNK2 enhancer methylation level.
- D Bar plots showing the loss of DNA methylation in the JNK2 enhancer region following a four-day treatment of PBMCs with cigarette smoke extract in 8 different donors.

Data information: (B, C) Box plots visualize 25/75 percentile and median, whiskers represent non-outlier range.

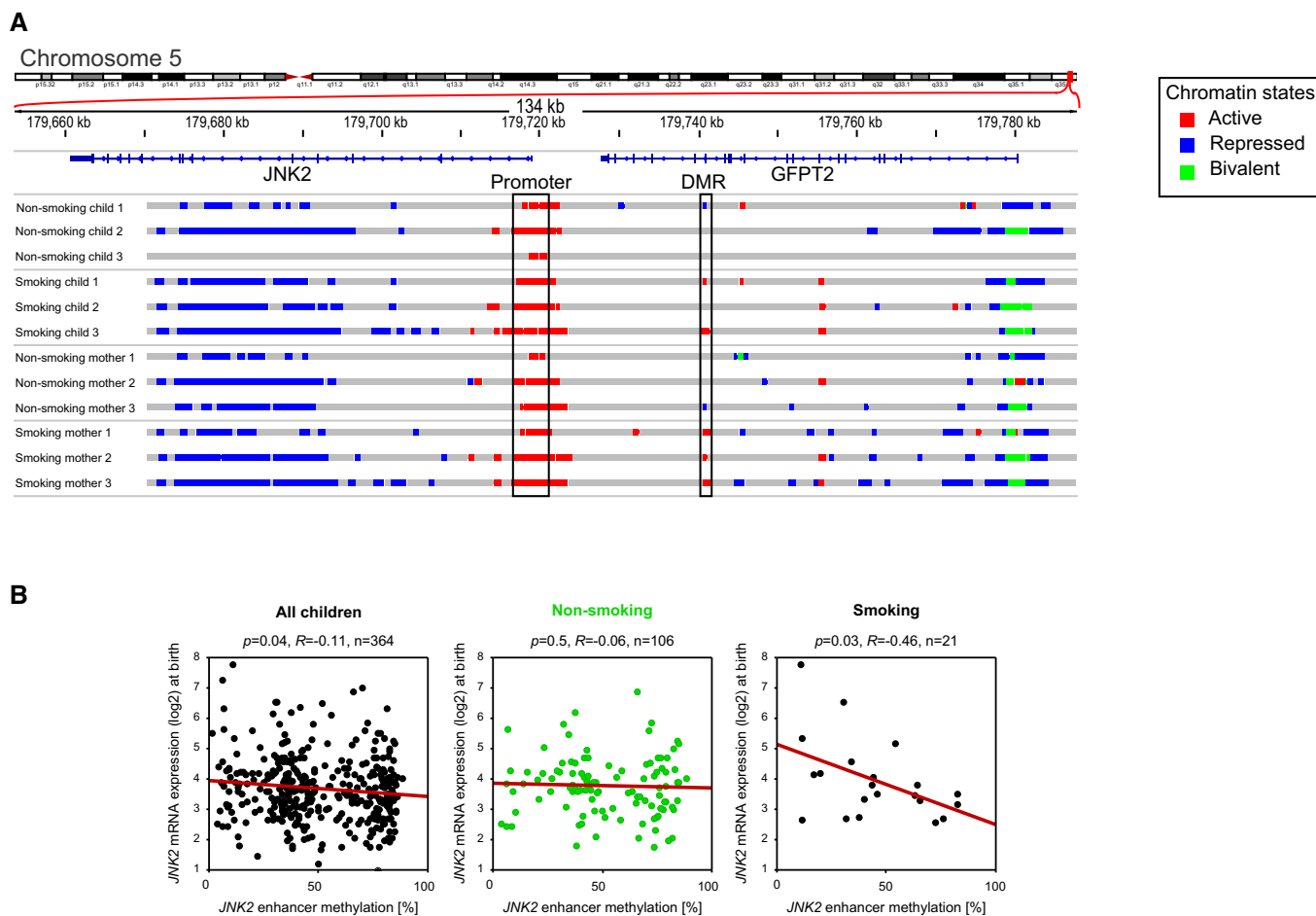


**Figure EV10. Example of the commuting JNK2 enhancer located in an intron of GFPT2.**

A Chromatin state comparison between non-smoking/smoking mothers and their children reveals a differentially active region in the intron of GFPT2, which corresponds to a hypomethylated gDMR in the smoking samples.

B Methylation of this region significantly, although weakly, correlates with gene expression of JNK2 ( $n = 364$ ). Considering children from non-smoking (urine cotinine [ $\mu\text{g}$ ]/creatinine [ $\text{g}$ ] < 1,  $n = 106$ ) or smoking mothers (urine cotinine [ $\mu\text{g}$ ]/creatinine [ $\text{g}$ ] > 100,  $n = 21$ ) separately reveals that a significant correlation of methylation and JNK2 transcription is observed only for children of smoking mothers corresponding to the differentially active characteristics of this region.

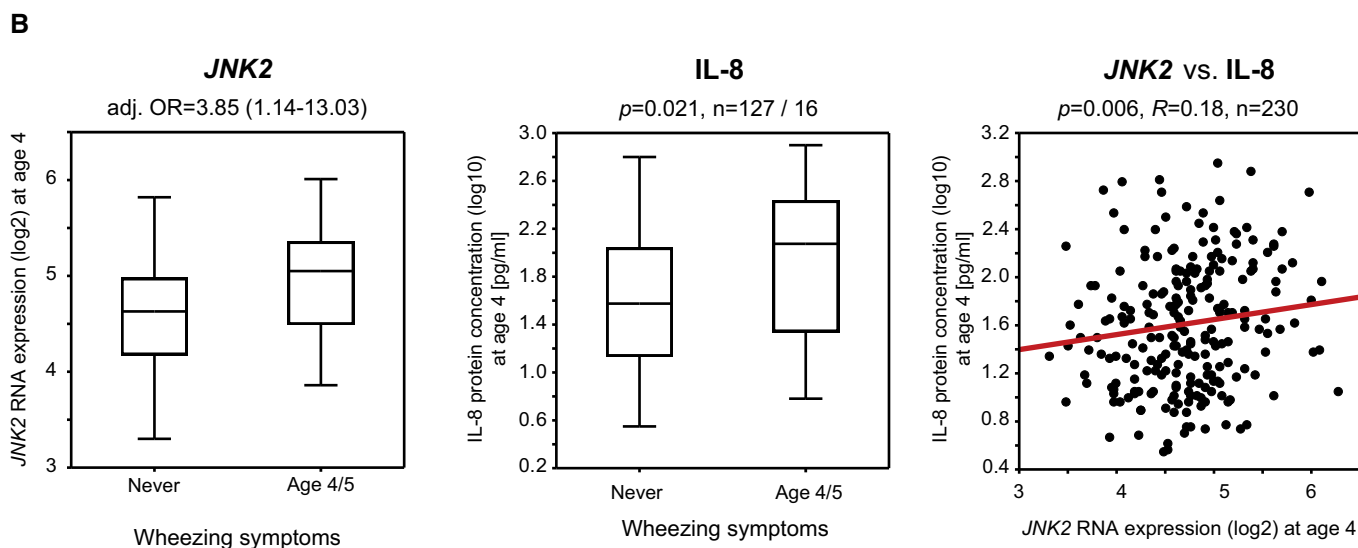
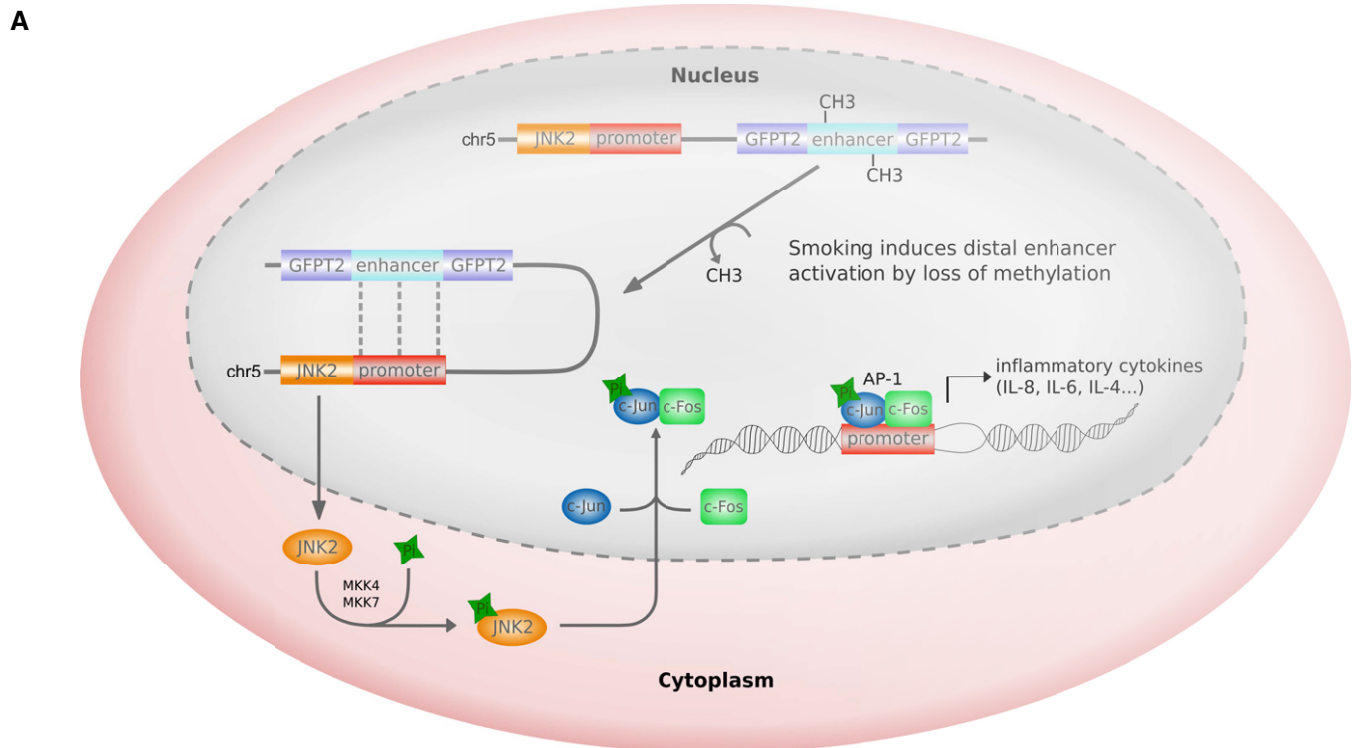


**Figure EV11. JNK2 deregulation and perturbed IL-8 secretion in wheezing children.**

**A** Loss of methylation in the differentially active JNK2 enhancer might contribute to differential JNK2 expression and altered secretion of the cytokine IL-8. JNK2 as a mediator of the early inflammatory response phosphorylates the transcription factor c-Jun that subsequently binds c-Fos, thereby forming the DNA-binding complex AP-1 (activator protein 1). AP-1 binding motifs have been identified in the promoter region of many cyto- and chemokines with IL-8 being one central downstream target.

**B** At age four, JNK2 gene expression and IL-8 protein concentration (measured in serum) are significantly elevated in wheezing children compared to those without any wheezing or other respiratory symptoms (Mann-Whitney test,  $P = 0.037$  and  $0.021$ , respectively). Both expression patterns correlate significantly in the entire cohort (Spearman's correlation  $p = 0.006$ , box plots visualize 25/75 percentile and median, whiskers represent non-outlier range).